

## NOTE

# Crystal structure of $\text{Ca}(\text{Fe}_{0.4}\text{Si}_{0.6})\text{O}_{2.8}$ oxygen-deficient perovskite

Masami KANZAKI<sup>1,†</sup><sup>1</sup>Institute for Planetary Materials, Okayama University, 827 Yamada, Misasa, Tottori 682–0193, Japan

The crystal structure of  $\text{Ca}(\text{Fe}^{3+}_{0.4}\text{Si}_{0.6})\text{O}_{2.8}$  oxygen-deficient perovskite phase synthesized at 12 GPa and 1400 °C was studied using synchrotron powder X-ray diffraction. The phase is isostructural to low-pressure phase of  $\text{Ca}(\text{Al}_{0.4}\text{Si}_{0.6})\text{O}_{2.8}$ . The structure was refined by the Rietveld method and consists of a perovskite-like triple-layer of corner-shared  $(\text{Fe}^{3+},\text{Si})\text{O}_6$  octahedra and a double-layer of  $\text{SiO}_4$  tetrahedra those are stacked alternatively in the [111] direction of ideal cubic perovskite. Small degree of  $\text{Fe}^{3+}/\text{Si}$  disorder was detected between two octahedral sites. The structure is compared with other oxygen-deficient perovskites.

©2020 The Ceramic Society of Japan. All rights reserved.

Key-words : Crystal structure, Rietveld refinement, Oxygen-deficient perovskite, High-pressure silicate

[Received June 17, 2020; Accepted July 29, 2020]

Oxygen-deficient perovskites are not only important for Ceramics Science, but also for Earth Science, since silicate perovskites are thought to be dominant constituent minerals in the Earth's deep mantle.<sup>1)</sup> Same crystal chemical principles can be applied for both silicate and non-silicate perovskites. There are several oxygen-deficient silicate perovskite phases exist in  $\text{CaSiO}_3$ – $\text{CaAlO}_{2.5}$  and  $\text{CaSiO}_3$ – $\text{CaFe}^{3+}\text{O}_{2.5}$  joins,<sup>2)</sup> and crystal structures of low-pressure phases of  $\text{Ca}(\text{Al}_{0.5}\text{Si}_{0.5})\text{O}_{2.75}$  and  $\text{Ca}(\text{Al}_{0.4}\text{Si}_{0.6})\text{O}_{2.8}$  were recently studied.<sup>3)</sup> They revealed that these phases consist of a perovskite-like layer and a double-layer of  $\text{SiO}_4$ , and the perovskite-like layer for  $\text{Ca}(\text{Al}_{0.5}\text{Si}_{0.5})\text{O}_{2.75}$  is made of two  $\text{AlO}_6$  octahedral layer, whereas that of  $\text{Ca}(\text{Al}_{0.4}\text{Si}_{0.6})\text{O}_{2.8}$  is made of tripe-layer of (Al,Si) octahedra. They suggested a homologous series in term of number of octahedral layers in perovskite-like layer for these oxygen-deficient silicate perovskites.

Unlike the  $\text{CaSiO}_3$ – $\text{CaAlO}_{2.5}$  join, only  $\text{Ca}(\text{Fe}^{3+}_{0.4}\text{Si}_{0.6})\text{O}_{2.8}$  phase is known as oxygen-deficient silicate perovskite phase in  $\text{CaSiO}_3$ – $\text{CaFeO}_{2.5}$  join.<sup>4)</sup> Although the  $\text{Ca}(\text{Fe}^{3+}_{0.4}\text{Si}_{0.6})\text{O}_{2.8}$  phase is likely isostructural to that of low-pressure  $\text{Ca}(\text{Al}_{0.4}\text{Si}_{0.6})\text{O}_{2.8}$ , no crystal structural study of the  $\text{Ca}(\text{Fe}^{3+}_{0.4}\text{Si}_{0.6})\text{O}_{2.8}$  phase has been conducted to date. In this study, crystal structure of the  $\text{Ca}(\text{Fe}^{3+}_{0.4}\text{Si}_{0.6})\text{O}_{2.8}$  was refined by the Rietveld method using synchrotron powder X-ray diffraction data.

Sample was synthesized using a Kawai-type double-stage multi-anvil high-pressure device driven by a 5000-ton press at the Institute for Planetary Materials (IPM). The starting material for the  $\text{Ca}(\text{Fe}_{0.4}\text{Si}_{0.6})\text{O}_{2.8}$  phase was prepared as follows. Firstly,  $\text{Ca}_2\text{SiO}_4$  was prepared by firing appropriate mixtures of reagent grade chemicals ( $\text{CaCO}_3$

and  $\text{SiO}_2$ ) at 1500 °C for 24 h. Then, a mixture of  $\text{Ca}_2\text{SiO}_4$ ,  $\text{Fe}_2\text{O}_3$ , and  $\text{SiO}_2$  with 5:2:1 molar ratio was prepared, and was used as starting material. For sample capsule, Au tube of 2.0 mm in outer diameter was used to avoid reaction with iron in the sample. In order to avoid reduction of  $\text{Fe}^{3+}$  to  $\text{Fe}^{2+}$  in the sample during high-pressure synthesis run, PdO powder was put at the bottom of Au sample tube, separated from the sample with a thin Pt foil. PdO is expected to release oxygen during the run. A Cr-doped MgO octahedral pressure cell (14M) assembly with a hBN– $\text{TiB}_2$  composite tube heater was employed.<sup>5)</sup>

The  $\text{Ca}(\text{Fe}^{3+}_{0.4}\text{Si}_{0.6})\text{O}_{2.8}$  phase was synthesized at about 12 GPa and 1400 °C for 3 h. The recovered sample was examined using a micro-focus X-ray diffractometer with a 100 μm beam diameter (RINT Rapid II, Rigaku Co.) for preliminary phase identification. This inspection revealed that the recovered sample mostly consists of the  $\text{Ca}(\text{Fe}^{3+}_{0.4}\text{Si}_{0.6})\text{O}_{2.8}$  phase, andradite ( $\text{Ca}_3\text{Fe}^{3+}_2\text{Si}_3\text{O}_{12}$ ) and larnite ( $\text{Ca}_2\text{SiO}_4$ ). This assemblage was consistent with the result of previous study<sup>4)</sup> obtained at similar pressures. Single phase was difficult to prepare. Thus, this mixture was used for synchrotron powder X-ray diffraction study. Synchrotron powder X-ray diffraction pattern of the recovered sample was obtained at the beamline BL19B2 of SPring-8. A large Debye–Scherrer camera with an imaging plate detector was used and the wavelengths of the X-ray beam used was 0.500052 Å, which was calibrated using  $\text{CeO}_2$  powder (NIST SRM 674b) with identical condition. The powdered sample was loaded into a glass capillary, which was rotated during the measurement. The exposure time was 10 min. RIETAN-FP program<sup>6)</sup> was employed for the Rietveld refinement using the diffraction patterns from 1.5 to 70.0° in  $2\theta$ . To avoid impurity peak, the pattern from 7.4 to 7.8° is excluded from the refinement. For andradite and larnite, structural parameters were fixed to

<sup>†</sup> Corresponding author: M. Kanzaki; E-mail: [mkanzaki@okayama-u.ac.jp](mailto:mkanzaki@okayama-u.ac.jp)

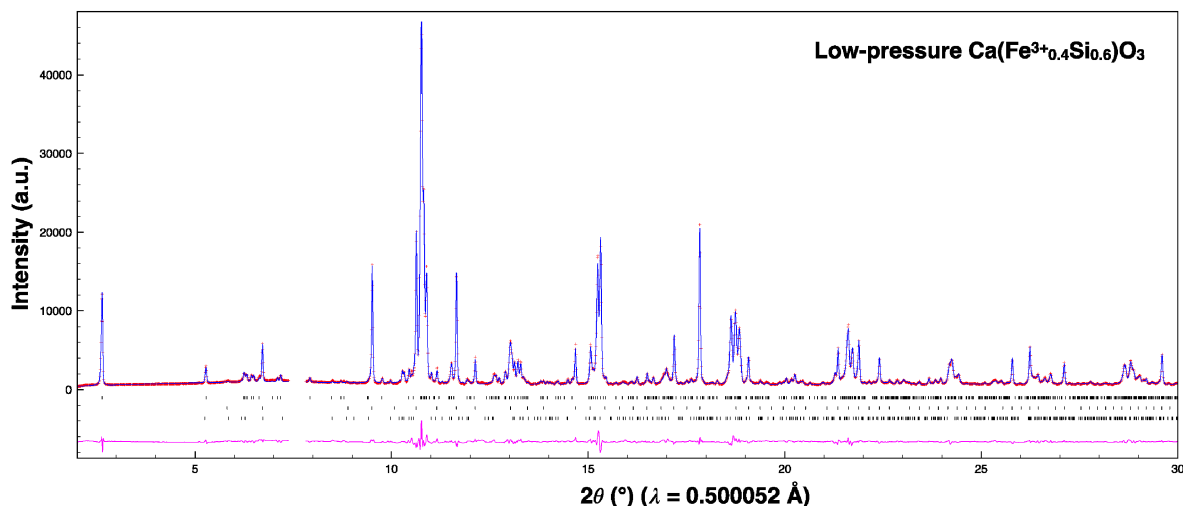


Fig. 1. Synchrotron powder X-ray diffraction pattern along with Rietveld refinement result of the  $\text{Ca}(\text{Fe}_{0.4}\text{Si}_{0.6})\text{O}_3$  sample synthesized at 12 GPa and 1400 °C. The observed intensities are shown by red crosses, and the calculated intensities are shown by a blue line. The line at the bottom is the difference between the observed and calculated intensities. Vertical ticks show positions of reflections of the  $\text{Ca}(\text{Fe}_{0.4}\text{Si}_{0.6})\text{O}_3$ , andradite and larnite (from top to bottom).

those reported ones, respectively.<sup>7,8)</sup> Only scale factor and cell parameters were refined for those phases. In order to check  $\text{Fe}^{3+}/\text{Si}$  disorder at two octahedral sites, occupancies for those sites were refined. Crystal structure is drawn by Vesta.<sup>9)</sup>

Powder X-ray diffraction pattern of the sample (Fig. 1) is similar to that of  $\text{Ca}(\text{Fe}^{3+}_{0.4}\text{Si}_{0.6})\text{O}_{2.8}$  phase plus andradite and larnite reported by the previous study conducted at similar pressure.<sup>4)</sup> The diffraction pattern from the  $\text{Ca}(\text{Fe}^{3+}_{0.4}\text{Si}_{0.6})\text{O}_{2.8}$  phase can be well correlated with those of low-pressure  $\text{Ca}(\text{Al}_{0.4}\text{Si}_{0.6})\text{O}_{2.8}$  phase,<sup>3)</sup> including the characteristic low-angle reflection at  $2.6^\circ$  ( $d = 10.86 \text{ \AA}$ ). Therefore this structure was refined by the Rietveld method using the crystal structure of low-pressure  $\text{Ca}(\text{Al}_{0.4}\text{Si}_{0.6})\text{O}_{2.8}$  phase as initial structure. The lattice parameters after Rietveld refinement are;  $a = 9.2727(2)$ ,  $b = 5.27291(11)$ ,  $c = 21.9357(5) \text{ \AA}$ ,  $\beta = 97.8775(10)^\circ$  ( $Z = 20$ ). These lengths are slightly (0.2–0.3 %) larger than those of previous report.<sup>4)</sup> Low-pressure  $\text{Ca}(\text{Al}_{0.4}\text{Si}_{0.6})\text{O}_{2.8}$  phase has the lattice parameters of  $a = 9.0365(2)$ ,  $b = 5.18766(12)$ ,  $c = 21.6291(5) \text{ \AA}$ ,  $\beta = 97.9987(9)^\circ$ ,<sup>3)</sup> and these lengths are smaller than those of  $\text{Fe}^{3+}$ -counterpart phase as a result of smaller Al ion replacing  $\text{Fe}^{3+}$ . The final  $R_{\text{wp}}$  and  $S$  for the pattern of the sample after refinement are 0.052 and 1.66, and the  $R_{\text{B}}$  and  $R_{\text{F}}$  for the phase are 0.024 and 0.028, respectively.

The powder X-ray diffraction pattern fitted by the Rietveld refinement is shown in Fig. 1. The resultant crystal structure is shown in Fig. 2, and the structural parameters and bond valence sum for each site are listed in Table 1. The cif file is deposited to COD (ID 3000276). The obtained structure confirms that the phase is isostructural to low-pressure  $\text{Ca}(\text{Al}_{0.4}\text{Si}_{0.6})\text{O}_{2.8}$  phase. Quantitative analysis of co-existing phases by the Rietveld refinement showed that the sample contained 69.1 wt %  $\text{Ca}(\text{Fe}^{3+}_{0.4}\text{Si}_{0.6})\text{O}_{2.8}$ , 26.0 wt % andradite ( $\text{Ca}_3\text{Fe}^{3+}_2\text{Si}_3\text{O}_{12}$ )

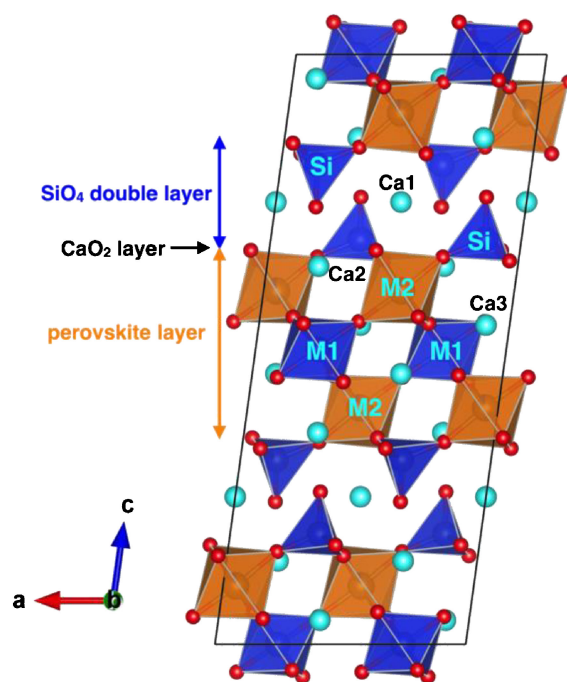


Fig. 2. Crystal structure of  $\text{Ca}(\text{Fe}_{0.4}\text{Si}_{0.6})\text{O}_{2.8}$  oxygen-deficient perovskite phase synthesized at 12 GPa and 1400 °C.

and 4.9 wt % larnite ( $\text{Ca}_2\text{SiO}_4$ ). Lattice parameters of larnite are within 0.3 % of reported values,<sup>8)</sup> thus there will be not much iron contamination in larnite.

For this  $\text{Ca}(\text{Fe}^{3+}_{0.4}\text{Si}_{0.6})\text{O}_{2.8}$  phase, the perovskite-like triple-layer is made of two kinds of octahedral sites. One octahedral site is locating at the middle of the triple-layer and is designated as M1 site in Fig. 2 and Table 1. Other is locating in upper and lower layers of M1 site and is designated as M2 site. For our previous study of low-pressure  $\text{Ca}(\text{Al}_{0.4}\text{Si}_{0.6})\text{O}_{2.8}$ ,  $^{29}\text{Si}$  and  $^{27}\text{Al}$  MAS NMR were used to probe Al/Si disorder in these M sites, as X-ray

**Table 1.** Structural parameters of  $\text{Ca}(\text{Fe}_{0.4}\text{Si}_{0.6})\text{O}_{2.8}$  oxygen-deficient perovskite phase synthesized at 12 GPa and 1400 °C

Atom	<i>x</i>	<i>y</i>	<i>z</i>	<i>B</i> /Å <sup>2</sup>	<i>BVS</i>
M1 <sup>#</sup>	1/4	1/4	1/2	0.21(2)	3.68
M2 <sup>#</sup>	0.0515(2)	0.2453(6)	0.90100(7)	0.21*	3.26
Ca1	0	0.8213(9)	1/4	1.53(10)	1.77
Ca2	0.7936(3)	0.7416(8)	0.64113(11)	0.69(4)	2.13
Ca3	0.4058(3)	0.7515(8)	0.45898(10)	0.90(5)	1.76
Si	0.6430(5)	0.7645(12)	0.18678(15)	1.08(7)	3.71
O1	0.8373(8)	0.2064(18)	0.2418(3)	1.41(5)	1.82
O2	0.8681(9)	0.538(2)	0.5549(4)	1.41 <sup>‡</sup>	1.97
O3	0.8037(9)	0.246(2)	0.6567(4)	1.41 <sup>‡</sup>	1.87
O4	0.9265(9)	0.4398(17)	0.8331(3)	1.41 <sup>‡</sup>	1.78
O5	0.8977(9)	0.7824(18)	0.4530(4)	1.41 <sup>‡</sup>	2.04
O6	0.9641(9)	0.0566(17)	0.3501(4)	1.41 <sup>‡</sup>	2.13
O7	0.1772(9)	0.0246(18)	0.9563(4)	1.41 <sup>‡</sup>	1.98

Note. Space group  $C2/c$ ;  $a = 9.2727(2)$ ,  $b = 5.27291(11)$ ,  $c = 21.9357(5)$  Å,  $\beta = 97.8775(10)^\circ$ ,  $Z = 20$ .  $R_{\text{wp}} = 5.15\%$ ,  $S = 1.66$ ,  $R_B = 2.37\%$ ,  $R_F = 2.80\%$ .

<sup>#</sup>: M1 = 0.827(2) Si + 0.173 Fe; M2 = 0.087 Si + 0.913 Fe

\*:  $B(\text{M1}) = B(\text{M2})$

<sup>‡</sup>: For all oxygen sites, *B* values were fixed to be equal.

*BVS*: bond valence sum. Bond valence parameters by Gagné and Hawthorne<sup>15)</sup> are used. For M1 and M2 sites, occupancy averaged values are given.

diffraction is not sensitive to distinguish Al and Si. Based on our previous study, M1 site is occupied by Si, whereas M2 is occupied by Al exclusively.<sup>3)</sup> For present study, we refined the occupancies of M sites. For M1 site, Si and Fe<sup>3+</sup> occupancies were 82.7 and 17.3 %, whereas they were 8.7 and 91.3 % for M2 site, respectively. Therefore, small degree of Fe<sup>3+</sup>/Si disorder exists on M sites, contrasting to Al-counterpart phase. These occupancies are supported from average bond distances for M sites. For M1 site, average bond distance is 1.842 Å, apparently longer than that for Si solely occupied octahedral sites. For example, average Si–O distance of MgSiO<sub>3</sub>-perovskite is 1.793 Å.<sup>10)</sup> This longer bond distance is consistent with some additional Fe<sup>3+</sup> in M1 site. On the other hand, average bond distance of 1.980 Å for M2 site is apparently smaller than expected for solely occupied Fe<sup>3+</sup> in octahedral sites. For example, Fe<sup>3+</sup>–O distance of andradite is 2.019 Å.<sup>7)</sup> Thus, those average bond distances confirm that there is some degree of Fe<sup>3+</sup>/Si disorder in M sites. Average bond distance for tetrahedral Si site was 1.657 Å and no apparent substitution of Fe<sup>3+</sup> to this site is expected. Mössbauer spectroscopic study<sup>4)</sup> of same phase has detected only octahedral Fe<sup>3+</sup>, consistent with present structure.

Bond valence sums for each site are given in Table 1. Except M1 and M2 sites, those sites are more or less close to the formal valences, suggesting no significant disorder. M1 and M2 sites have values between 3 and 4 as a result of Fe<sup>3+</sup>/Si disorder discussed before.

There are three Ca sites. Ca1 site has largest isotropic displacement parameter than other two Ca sites. Ca1 site is locating in CaO<sub>2</sub> layer where one oxygen is deficient from ideal perovskite's CaO<sub>3</sub> close packed layer.<sup>3),11)–12)</sup> Ca1 site is coordinated by eight oxygens with average bond distance of 2.528 Å (cutoff distance = 2.7 Å). Ca3 site is

locating inside of the perovskite triple-layer, so its local environment is supposed to similar to that of perovskite structure without oxygen-deficiency. However, this site is coordinated by six oxygens with average bond distance of 2.479 Å if cutoff distance of 2.7 Å is applied. There are five more oxygens with bond distances below 3 Å. Thus, Ca3 site is more distorted. Ca2 site is somewhat between former two and is coordinated by eight oxygens with average bond distance of 2.497 Å below 2.7 Å cutoff, but there is ninth oxygen at 2.880 Å. Those coordination numbers are lower than that of ideal perovskite (12).

Known oxygen-deficient silicate perovskites to date have common structural features. They have double SiO<sub>4</sub> layer in which SiO<sub>4</sub> is isolated from each other. Perovskite-like octahedral layers are also indispensable. Number of octahedral layers are variable, and  $n = 1$  (BaCa<sub>2</sub>MgSi<sub>2</sub>O<sub>8</sub>),<sup>14)</sup> 2 [Ca(Al<sub>0.5</sub>Si<sub>0.5</sub>)O<sub>2.75</sub>], and 3 [Ca(Fe<sup>3+</sup><sub>0.4</sub>Si<sub>0.6</sub>)O<sub>2.8</sub>] are known.<sup>3)</sup> These layers stacked to [001] direction of cubic perovskite. Although many oxygen-deficient perovskite (and related) structures are known,<sup>11),12)</sup> as far as we are aware, this combination is not known for non-silicates. Why more common structures are not realized in oxygen-deficient silicate perovskites is considered here. The double-tetrahedral layer is resulted from formation of CaO<sub>2</sub> layer (or AO<sub>2</sub> layer in general where large divalent cation A = Ba, Sr, Ca). It is possible to have AO layer by taking away two oxygens from ideal AO<sub>3</sub> layer. For example, Ba<sub>2</sub>InAlO<sub>5</sub> has the AO layer resulting a double tetrahedral AlO<sub>4</sub> layer, but AlO<sub>4</sub> tetrahedra in this case share one corner.<sup>13)</sup> Therefore, analogous Ca<sub>2</sub>MgSiO<sub>5</sub> phase could be realized. However, this phase will not be stable, as Si–O–Si angle of 180° by corner-shared SiO<sub>4</sub> tetrahedra should be formed. This angle is unfavored for silicates. This could be a reason for non-existence of this type of structure with AO oxygen-defect layer. The AO<sub>2</sub> layer-containing structures exist in Ba-manganates and Ba-cobaltates for example,<sup>12)</sup> but octahedral layers contain face-shared octahedra rather than only edge-shared ones. Face-shared octahedra are apparently avoided for relatively high valence cations such as Si<sup>4+</sup>. Again, such structures are unfavored for silicates.

Although present consideration cannot fully explain many aspects of structure of oxygen-deficient silicate perovskites, crystal chemical insights are useful to understand oxygen-deficient perovskite structures appeared in both Ceramic Science and Earth Science fields.

**Acknowledgements** Synchrotron Powder X-ray diffraction pattern was measured at BL19B2 of SPring-8 (Proposal No. 2012B1930). The study was supported by Operational Expenses Grant from Okayama University.

## References

- 1) A. Navrotsky, *Science*, **284**, 1788–1789 (1999).
- 2) U. W. Bläß, F. Langenhorst, D. J. Frost and F. Seifert, *Phys. Chem. Miner.*, **34**, 363–376 (2007).
- 3) M. Kanzaki, X. Xue, Y. Wu and S. Nie, *Phys. Chem. Miner.*, **44**, 717–733 (2017).

- 4) U. W. Bläß, F. Langenhorst, T. Boffa-Ballaran, F. Seifert, D. J. Frost and C. A. McCammon, *Phys. Chem. Miner.*, **31**, 52–57 (2004).
- 5) M. Kanzaki, *Am. Mineral.*, **95**, 1349–1352 (2010).
- 6) F. Izumi and K. Momma, *Solid State Phenom.*, **130**, 15–20 (2007).
- 7) R. M. Hazen and L. W. Finger, *Am. Mineral.*, **74**, 352–359 (1989).
- 8) T. Tsurumi, Y. Hirano, H. Kato, T. Kamiya and M. Daimon, *Ceram. Trans.*, **40**, 19–25 (1994).
- 9) K. Momma and F. Izumi, *J. Appl. Crystallogr.*, **44**, 1272–1276 (2011).
- 10) H. Horiuchi, E. Ito and D. J. Weidner, *Am. Mineral.*, **72**, 357–360 (1987).
- 11) J. Darriet and M. A. Subramanian, *J. Mater. Chem.*, **5**, 543–552 (1995).
- 12) R. J. D. Tilley, *Perovskites: Structure-Property Relationships*, pp. 316, John Wiley & Sons, U.K. (2016).
- 13) H. Müller-Buschbaum and M. Abed, *Z. Anorg. Allg. Chem.*, **591**, 174–180 (1990).
- 14) C.-H. Park, T.-H. Kim, Y. Yonesaki and N. Kumada, *J. Solid State Chem.*, **184**, 1566–1570 (2011).
- 15) O. C. Gagné and F. C. Hawthorne, *Acta Crystallogr. B*, **71**, 562–578 (2015).